

Characterization of calcium oxide derived from waste eggshell and its application as CO₂ sorbent

Thongthai Witoon^{a,b,*}

^a National Center of Excellence for Petroleum, Petrochemicals and Advance Material, Department of Chemical Engineering, Faculty of Engineering, Kasetsart University, Bangkok 10900, Thailand

^b Center for Advanced Studies in Nanotechnology and Its Applications in Chemical Food and Agricultural Industries, Kasetsart University, Bangkok 10900, Thailand

Received 10 May 2011; accepted 24 May 2011

Available online 30 May 2011

Abstract

The carbonation–calcination looping cycle of calcium-based sorbents is considered as an attractive method for CO₂ capture from combustion gases because it can reduce the cost during the capture steps compared to conventional technologies, e.g., solvent scrubbing. In this study, waste eggshell was used as raw material for calcium oxide-based sorbent production. The commercially available calcium carbonate was employed for comparison purpose. Calcination behavior, crystal type and crystallinity, surface chemistry, qualitative and quantitative elemental information, specific surface area and pore size, morphology of the waste eggshell and the calcined waste eggshell were characterized by thermal gravimetric analysis (TGA), X-ray diffraction (XRD), Fourier transform infrared spectroscopy (FT-IR), X-ray fluorescence (XRF), N₂ sorption analysis and scanning electron microscopy (SEM), respectively. The carbonation–calcination cycles were carried out using a TGA unit with high purity CO₂ (99.999%). It was found that the carbonation conversion of the calcined eggshell was higher than that of the calcined commercially available calcium carbonate after several cycles at the same reaction conditions. This could be due to the fact that the calcined eggshell exhibited smaller particle size and appeared more macropore volume than the calcined commercially available calcium carbonate. As results, the calcined eggshell provided a higher exposed surface for the surface reaction of CO₂.

© 2011 Elsevier Ltd and Techna Group S.r.l. All rights reserved.

Keywords: A. Sintering; C. Chemical properties; Eggshell; Calcium oxide; CO₂ sorbent; CO₂ capture

1. Introduction

The problem of global warming caused by CO₂ emission has raised serious concerns since the CO₂ concentration in the atmosphere has increased rapidly due to the industrial revolution. The reduction of CO₂ emission can occur as a result of increased energy efficiency [1,2], substitution of non-carbon fuels [3] or by the capture and storage of CO₂ [4,5]. With the United Nations predicting world population growth from 6.6 billion in 2007 to 8.2 billion by 2030, demand for energy must increase substantially over that period [6] which no doubt erase gains associated with increased energy efficiency. Fossil

fuels will continue to be major source of energy for the next few decades because the non-carbon energy sources still are more limited and more expensive. Thus, the capture and storage of CO₂ will be required in order to allow us to utilize fossil fuels without CO₂ emission.

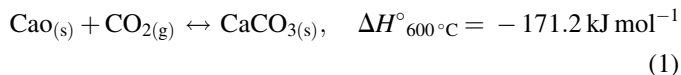
The current commercial operation for CO₂ capture used a chemical absorption method with Monoethanol Amine (MEA) as the sorbent has been recognized as the most matured process [7]. The chemical interaction between the MEA and the CO₂ molecules is strong and this offers a fast and effective removal of the CO₂ in one stage of absorption. However, the strong interaction between the MEA and the CO₂ molecules requires important amounts of energy to regenerate the MEA solution. The MEA is highly corrosive leading to the use of costly absorber packing and column materials. Finally, the impurities and minor components in the flue gas including SO₂, NO₂, O₂, etc. have to be removed before the gas enters the absorber in order to prevent the degradation of the MEA solution. This

* Correspondence address: National Center of Excellence for Petroleum, Petrochemicals and Advance Material, Department of Chemical Engineering, Faculty of Engineering, Kasetsart University, Bangkok 10900, Thailand. Tel.: +66 2579 2083; fax: +66 2561 4621.

E-mail address: fengtwi@ku.ac.th.

requires several pretreatment processes and therefore leads to high capture costs estimated at around 59.1\$/tonnes of CO₂ avoided [7]. Many researchers have focused on the development of new absorbents to increase in the CO₂ absorption rate. Rivera-Tinoco and Bouallou [8] demonstrated that the CO₂ absorption by ammonia was faster than that carried out by N-methyldiethanolamine (MDEA). Various strategies for minimizing the energy requirements from the chemical absorption method have been investigated and proposed. Harkin et al. [9] combined pinch analysis and linear programming optimization for the energy requirements of power plants. They found that the effective heat integration can reduce the energy requirements by up to 50%. Nevertheless, the CO₂ capture by means of amines may be not suitable since some of the amines escaping the recycling process will be emitted into the air and will also form other compounds such as nitrosamines and nitramines which can affect health and environment [10]. It is therefore essential to develop technologies that can reduce the cost of carbon capture with environment friendly.

The use of calcium oxide (CaO) for CO₂ looping cycle has attracted increasing attention due to a number of its potential advantages, including a wide range of potential operating temperatures, reduction of energy requirement, elimination of the generation of liquid wastes, and the relatively inert nature of solids wastes [11]. The application of CaO is basically through carbonation–calcination cycles with CO₂ based on the reversible reaction (Eq. (1)).



The major challenge of this cycle in practical applications is a sharp decay after few cycles of carbonation–calcination. The deactivation of CaO-based CO₂ sorbents is caused by the sintering process due to three majors factors: (1) the carbonation is highly exothermic; (2) there is a volumetric expansion from CaO to CaCO₃ (from 16.9 to 34.1 cm³/mol), which significantly decreases the distance between particles in the carbonated state; (3) CaCO₃ has a Tammann temperature of 533 °C, lower than normal carbonation temperature [12]. Recently, several strategies have been studied to overcome those problems, including: (1) decreasing CaO particle size [13]; (2) synthesizing new CaO-based mesoporous silica [14]; (3) improving the porosity of CaO by hydration treatment [15]; (4) enhancement of reactivity using surfactant-modified CaO [16]; (5) addition of inert phase such as potassium, sodium, compounds of titanium, KMnO₄-doped CaO, MgO-doped CaO, La₂O₃-doped CaO [17–20]; (6) using other calcium-based natural minerals, such as dolomite and huntite [21]. Besides, there are several natural calcium sources from wastes, such as mussel shell, scallop shell, mollusk shell, and eggshell.

Eggs represent a major ingredient in a large variety of products such as cakes, salad dressings and fast foods, whose production results in several daily tons of waste eggshell and incur considerable disposal costs in Thailand. The disposal of the waste is a very important problem, which can cause risk to public health, contamination of water resources and polluting the

environment. Based on the cleaner production concepts [22], the use of wastes to be the CO₂ sorbent not only provides the technology with competitive sorbent processing costs but also eliminate the wastes simultaneously. To the best of my knowledge, very few researches on the use of waste eggshell as the CO₂ sorbent have been reported [23]. In this work, CaO derived from waste eggshell were thoroughly investigated by using thermogravimetric analysis (TGA), X-ray diffraction, X-ray fluorescence, Fourier transform infrared (FTIR) spectroscopy, nitrogen sorption measurement, scanning electron microscopy (SEM). CO₂ adsorption capacity of the CaO derived from waste eggshell was measured by gravimetric method at different temperatures. Durability test of the CaO derived from waste eggshell was conducted. The similar experiments were repeated with the commercially available CaCO₃ for comparison purpose.

2. Materials and methods

2.1. Materials

Waste eggshell sample was collected from canteen, Kasetsart University, Bangkok, Thailand. The sample was washed several times with deionized water to remove additional residues from its surface, filtered with 0.45 μm membrane filter and then dried at 105 °C for 24 h. The commercially available calcium carbonate (CaCO₃) was purchased from Ajax Finechem for comparison. The samples were pulverized and sieved in the range of 250–425 μm. The obtained samples were calcined at 900 °C for 1 h under N₂ atmosphere.

2.2. Characterization

The weight change and the calcination temperature of dried eggshell were investigated by using DSC-TGA 2960 thermal analyzer in a flow of nitrogen atmosphere at a heating rate of 10 °C/min. The sample loading was typically 20–25 mg.

X-ray fluorescence (PANalytical Epsilon 5) was used for the qualitative and quantitative analysis of the inorganic compounds in the natural and the calcined eggshell.

X-ray diffraction (XRD) patterns of the dried eggshell, the calcined eggshell and the calcined CaCO₃ were done on a diffractometer (Bruker D8 Advance) using Cu-K_α radiation. The measurements were made at room temperature at a range of 15–70 °C on 2θ with a step size of 0.05°. The diffraction patterns were analyzed using the Joint Committee on Powder Diffraction Standards (JCPDS). CaO crystallite size was calculated using Scherrer equation from the most intense CaO peak at 2θ of 37.4° as shown below:

$$d = \frac{0.89\lambda}{B \cos \theta} \times \frac{180^\circ}{\pi} \quad (2)$$

where *d* is the mean crystallite diameter, λ is the X-ray wave length (1.54 Å), and *B* is the full width half maximum (FWHM) of the CaO diffraction peak.

Fourier transform infrared (FTIR) spectra were obtained by using spectrophotometer (Bruker Tensor 27) in the range of

400–4000 cm^{-1} with a resolution of 4 cm^{-1} . The sample preparation consisted of mixing fine powder of each sample dried eggshell, calcined eggshell and calcined CaCO_3 with KBr powder.

N_2 adsorption–desorption isotherms of the samples were measured at -196°C using a Quantachrome Autosorb-1C instrument. Prior to measurements, the samples were degassed at 105°C for 24 h. Pore size distributions of the samples were determined from the adsorption branch of the isotherms by the Barrett–Joyner–Hallenda (BJH) method. The specific BET (S_{BET}) was estimated for P/P_0 values between 0.05 and 0.30. The pore volume was reported as mesopore (2–50 nm) and macropore (>50 nm) volumes.

The morphologies and dimensions of the samples were observed by scanning electron microscope (SEM; Philips XL30). SEM was operated at 14.0 kV of an accelerating voltage. The samples were sputter-coated with gold prior to analysis.

2.3. CO_2 carbonation–calcination performance tests

CO_2 carbonation–calcination measurements were performed for all CaO products by using a SDT2960 simultaneous DTA–TGA Universal 2000. A 20–25 mg sample was loaded into an alumina sample pan. Prior to any CO_2 carbonation–calcination experiment and to remove pre-adsorbed CO_2 and H_2O , the sample was first activated by heating it from room temperature in a flow of pure N_2 (100 mL/min) at a rate of $20^\circ\text{C}/\text{min}$ until 900°C was achieved and the sample was kept at 900°C for 5 min; then the sample was cooled to a given temperature (650, 700 and 750°C). Once the carbonation temperature was reached and stabilized, pure CO_2 (99.999%) with a flow rate of 80 mL/min was introduced into the system while the change in the sample weight was recorded. After the carbonation for 50 min, the CO_2 flow was disconnected and the N_2 flow was subsequently introduced. The sample was heated to 900°C at a rate of $20^\circ\text{C}/\text{min}$ and kept at 900°C for 5 min to complete conversion to CaO. After calcination process, the sample was cooled down to a given temperature again (650, 700 and 750°C) for carbonation process. The same experiment was repeated 11 times in order to investigate the performance of the reversibility and stability of CO_2 carbonation–calcination. The carbonation conversion is calculated as follows:

$$X_n = \frac{m_{\text{carb}}^n - m_{\text{cal}}^n}{m_0 a} \times \frac{W_{\text{CaO}}}{W_{\text{CO}_2}} \quad (3)$$

where X_n is the carbonation conversion of the sorbent after n cycles, m_0 is the initial mass of the sorbent, a is the content of CaO in the initial sorbent, m_{carb}^n is the mass of the carbonated sorbent after n cycles, m_{cal}^n is the mass of the calcined sample after n cycles. W_{CaO} and W_{CO_2} are the molar masses of CaO and CO_2 , respectively. The carbonation rate is defined as follows:

$$r_n = \frac{dX_n}{dt} \quad (4)$$

where r_n is the carbonation rate after n cycles and t is the carbonation time at each cycle.

3. Results and discussion

3.1. Characterization

The suitable calcination temperature of eggshell was analyzed by TGA/DTA. As shown in Fig. 1, the TGA pattern of dried eggshell showed two distinct stages of weight losses: one at temperature below 680°C and one between 680 and 850°C . The first stage can be attributed to adsorbed water molecules and loss of organic compounds. The second stage exhibited the major weight loss at 830°C , corresponding to 42 wt.% was due to the change of CaCO_3 phase to CaO phase which could be confirmed by the XRD and the FTIR results (Figs. 2 and 3). As the sample weight remained constant after 850°C , the temperature of 900°C was then suitable for the use as the calcination temperature to ensure complete conversion to CaO.

X-ray diffraction pattern of dried eggshell (Fig. 2a) shows a major peak at $2\theta = 29.5^\circ$, indicating that calcite (CaCO_3) is a major phase of the waste eggshell. CaO phase with 2θ values of 32.3° , 37.4° , 53.9° , 64.2° and 67.4° was found when the eggshell was calcined at 900°C for 1 h (Fig. 2b). The major peak of calcite phase ($2\theta = 29.5^\circ$) was not shown in XRD pattern of the calcined eggshell, implying that the CaCO_3 phase was completely transformed to CaO phase. XRD pattern of the

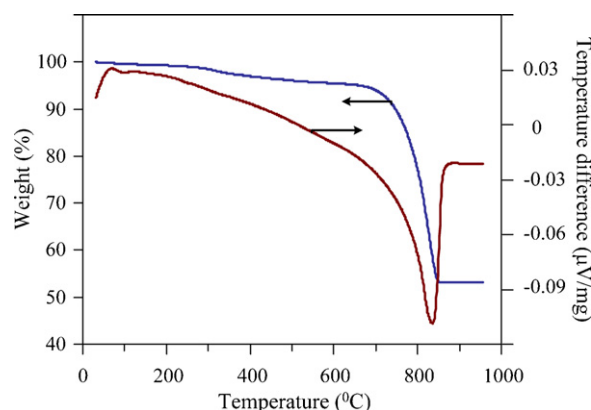


Fig. 1. TGA–DTA pattern of dried eggshell (DES).

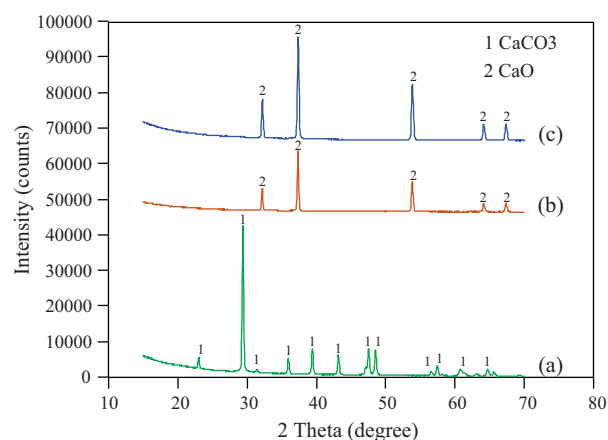


Fig. 2. XRD patterns of dried eggshell (a), calcined eggshell (b) and calcined commercially available CaCO_3 (c).

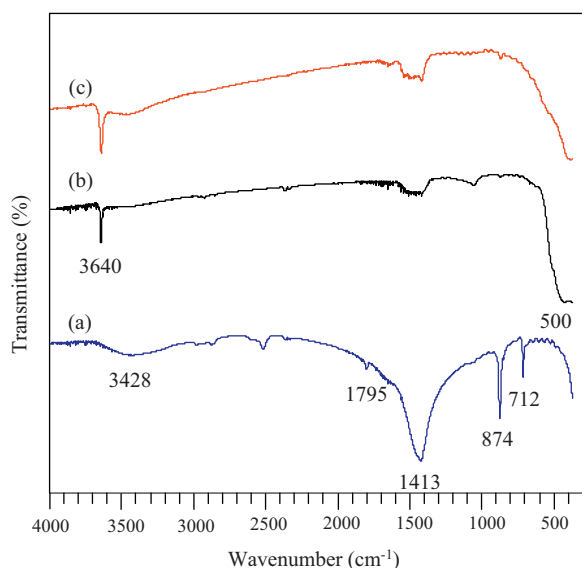


Fig. 3. FTIR spectra of dried eggshell (a), calcined eggshell (b) and calcined commercially available CaCO_3 (c).

calcined commercially available CaCO_3 (Fig. 2c) appeared at the same 2θ angles as that of the calcined eggshell. However, the peaks intensities of the calcined commercially available CaCO_3 were higher than those of the calcined eggshell, suggesting that the CaO crystalline size of the calcined commercially available CaCO_3 was larger than that of the calcined eggshell. The CaO crystallite size calculated by using Scherrer equation is listed in Table 1. It was found that the calcined eggshell generated the nanocrystalline CaO with a crystallite size of 44.3 nm, while the calcined commercially available CaCO_3 showed a very high degree of crystallinity with a crystallite size of more than 100 nm.

The usefulness of qualitative analysis from the characteristic frequencies provides information to identify chemical constituents in a compound. Fig. 3a shows the IR spectra of the dried eggshell. The broad transmission band at approximately 3428 cm^{-1} can be attributed to OH stretching vibration from residual water. The weak band at 1795 cm^{-1} corresponds to $\text{C}=\text{O}$ bonds from carbonate. Two well-defined infrared bands at 1413 and 873 cm^{-1} are characteristic of the $\text{C}-\text{O}$ stretching and bending modes of calcium carbonate, respectively [24]. The sharp band at 712 cm^{-1} is related to $\text{Ca}-\text{O}$ bonds [25]. Fig. 3b shows the spectrum of the calcined eggshell. The existence of peak at 3640 cm^{-1} is due to OH in $\text{Ca}(\text{OH})_2$ formed during

Table 1
Physical properties and CaO crystallite size of different samples.

Sample ^a	BET surface area (m^2/g)	Mesopore volume (cm^3/g)	Macropore volume (cm^3/g)	CaO crystallite size (nm)
DES	0.05	0.001	0.007	—
CES	13.45	0.007	0.021	44.3
CCA	19.04	0.030	0.001	102.1

^a Dried eggshell, calcined eggshell and calcined commercially available CaCO_3 are designated as DES, CES and CCA, respectively.

Table 2

Chemical composition of calcined eggshell (wt.%).

Sample	CaO	MgO	P_2O_5	SO_3	K_2O	SrO	Cl	Fe_2O_3	CuO
Calcined eggshell	97.42	1.63	0.52	0.26	0.08	0.05	0.02	0.01	0.01

adsorption of water by CaO . The wide and strong band at around 500 cm^{-1} corresponds to the $\text{Ca}-\text{O}$ band. The IR spectrum of the calcined commercially available CaCO_3 (Fig. 3c) appeared at the same wavenumber of the calcined eggshell, indicating that the calcined eggshell and the calcined commercially available CaCO_3 have a very similar chemical nature.

The chemical composition of the calcined eggshell (Table 2) shows that the CaO is the most abundant component (97.4%). The high amount of calcium oxide is associated with the presence of the calcium carbonate, which is the main component of the waste eggshell confirmed by the XRD and FTIR results. The calcined eggshell only contained small amounts of MgO , P_2O_5 , SO_3 , K_2O , SrO , Fe_2O_3 , CuO . Thus, the waste eggshell can be

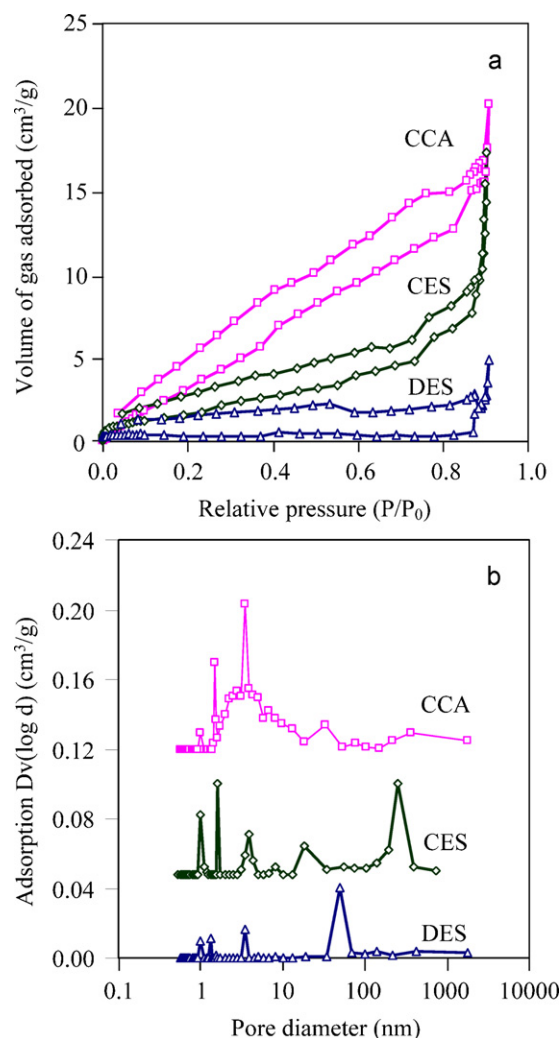


Fig. 4. N_2 sorption isotherms (a) and pore size distributions (b) of dried eggshell (DES), calcined eggshell (CES) and calcined commercially available CaCO_3 (CCA).

considered from a chemical viewpoint as a pure relatively natural carbonate-based material.

Due to the fact that the characteristics of the pore structure of CaO strongly influences on the diffusion and reaction of CO₂, therefore they must be thoroughly investigated and reported. The pore characteristics of all samples measured by N₂-physisorption are shown in Fig. 4. The physical properties including BET surface area, mesopore volume and macropore volume are given in Table 1. As shown in Fig. 4a, the isotherms of all samples exhibited type IV–II composite isotherms which is the characteristic of mesoporous–macroporous material. However, the amount of gas adsorbed of each sample was quite

different. The isotherm of the dried eggshell was almost parallel to the *x*-axis, showing no multilayer gas adsorption. This observation indicated that the dried eggshell sample should contain only macropore without the significant contribution of mesopore volume. After calcination, the amount of gas adsorbed was increased, suggesting that numerous pores were created. Comparing between the calcined eggshell and the calcined commercially available CaCO₃ at relative pressure range of 0.2–0.8, the amount of gas adsorbed of the calcined eggshell was lower than that of the calcined commercially available CaCO₃, indicating that the calcined commercially available CaCO₃ had higher amount of mesopores and BET

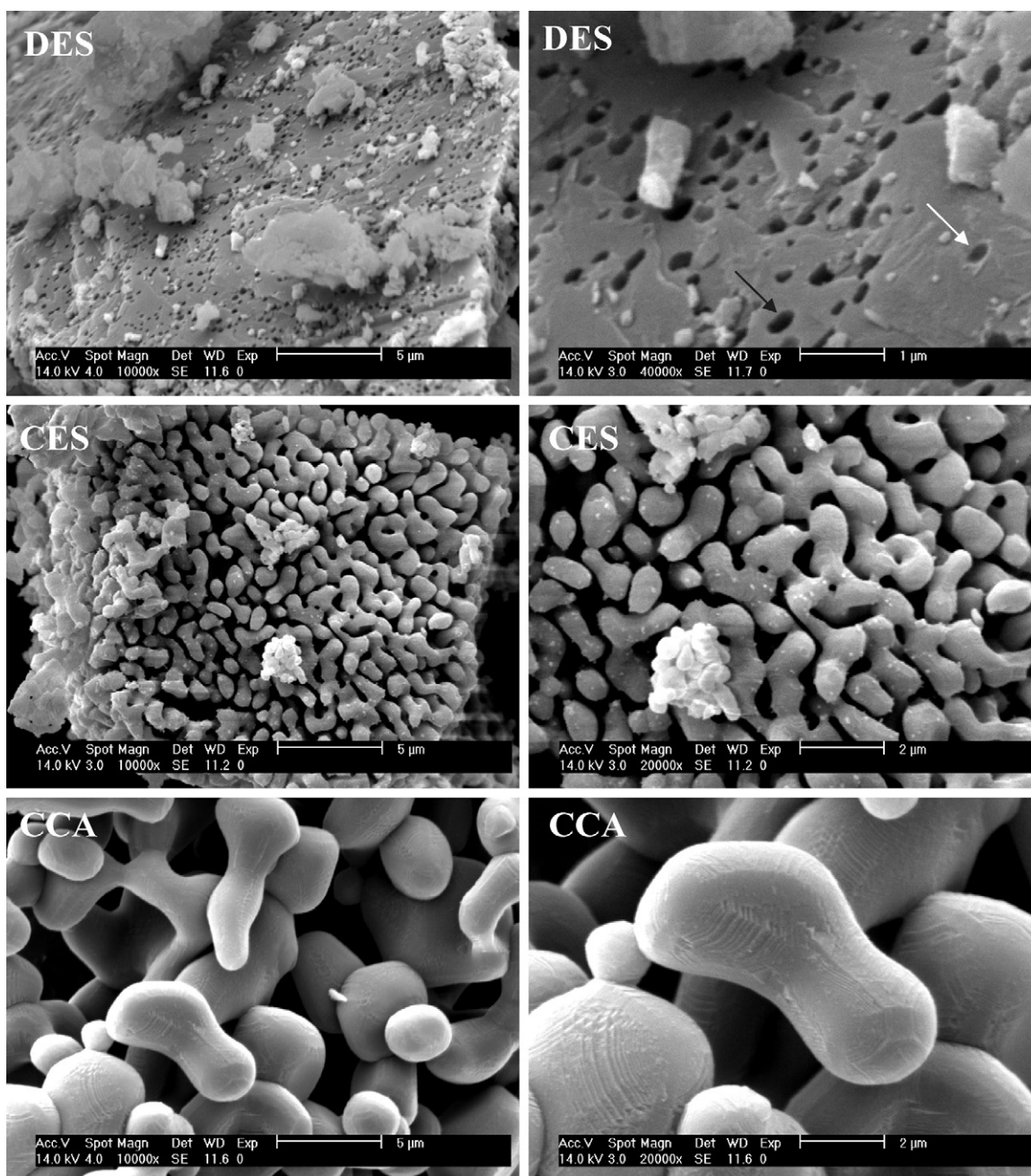


Fig. 5. SEM images of dried eggshell (DES), calcined eggshell (CES) and calcined commercially available CaCO₃ (CCA) at low (left) and high (right) magnifications.

surface area. However, the opposite trend was observed at relative pressure higher than 0.85, implying that the calcined eggshell had higher macropores.

The pore size distributions of all samples calculated by BJH adsorption method are shown in Fig. 4b. It was found that the pore size distribution of the dried eggshell sample is multi-modal size, with mean pore diameters of 1.0 nm, 1.3 nm and 50 nm. After calcination, some pore sizes are shifted to larger pore size and the volume of those pores are significantly increased. This is due to the fact that the removal of CO_2 during calcination process creates small pores, whereas the larger pores are obtained by the aggregates of the large grain size formed by the sintering of the smaller ones. Moreover, the small pores can possibly merge each other to form larger ones. The calcined commercially available CaCO_3 possess more porosity in the range of mesopore region (2–50 nm). The foregoing observations are consistent with the results in Table 1.

The apparent morphologies of the dried eggshell, the calcined eggshell and the calcined commercially available CaCO_3 examined by SEM are shown in Fig. 5. The dried eggshell was irregularly and very finely undulated. There were many pores and pits distributed over the entire eggshell surface. The size of the pores and the pits varied randomly from place to place. After calcination, the structure of the dried eggshell has been changed from the irregular crystal structure to interconnected skeleton structure. The size of the skeletons was found to be approximately 1–3 μm . The voids between these skeletons were in excess of 500 nm, which eluded measurement with N_2 -physisorption. It was clearly seen that the skeleton size and the voids of the calcined eggshell was smaller than those of the calcined commercially available CaCO_3 . This was in good agreement with the CaO crystallite size obtained by the XRD results. However, it should be noted that the skeleton size observed by the SEM images was larger than the crystallite size obtained by the XRD results because the skeleton was formed by the aggregates of several nanocrystallites.

3.2. CO_2 capture performance

The carbonation conversions and carbonation rates of the calcined eggshell and the calcined commercially available CaCO_3 at different carbonation temperature are shown in Fig. 6. It is found that the carbonation of the two sorbents obviously occurs in two stages. The first stage rapidly occurs within 3 min due to the fast reaction of CO_2 on the outer surface of CaO particle to form the CaCO_3 layer covering the CaO core. The formation of CaCO_3 layer increases the diffusion resistance of CO_2 to react with the CaO core and thus reduces the reaction rate which is the second stage of the reaction. It can be clearly seen that the carbonation conversion of the sorbents is increased with increasing the carbonation temperature except that of CCA-750. Based on the reaction kinetics, both the reaction and solid-state diffusion rates are enhanced with the increase in the temperature. It should be noted, however, that the carbonation conversion of the CES sorbent at 750 $^\circ\text{C}$ is slightly higher than that at 700 $^\circ\text{C}$ and the difference of the carbonation conversions tends to be small with the increase of

the carbonation time. Similar result is also observed for the CCA sorbent. The conversion of CCA sorbent at 750 $^\circ\text{C}$ is lower than that at 700 $^\circ\text{C}$ after 20 min of the carbonation time. This could be explained by the competition between the forward and reverse reactions (Eq. (1)), the particle size of the sorbents as well as the carbonation times.

It can be clearly seen that the carbonation conversion of the calcined eggshell is twice higher than that of the calcined commercially available CaCO_3 compared at the same carbonation temperature. The better carbonation performance of the calcined eggshell relative to that of the calcined commercially available CaCO_3 can be attributed to the smaller crystal grain size of the calcined eggshell, which provided a larger exposed surface area for the interaction between CaO and CO_2 and also produced a thinner layer of CaCO_3 , resulting in the easier diffusion of CO_2 .

In order to compare the durability performance of the calcined eggshell (CES) and the calcined commercially

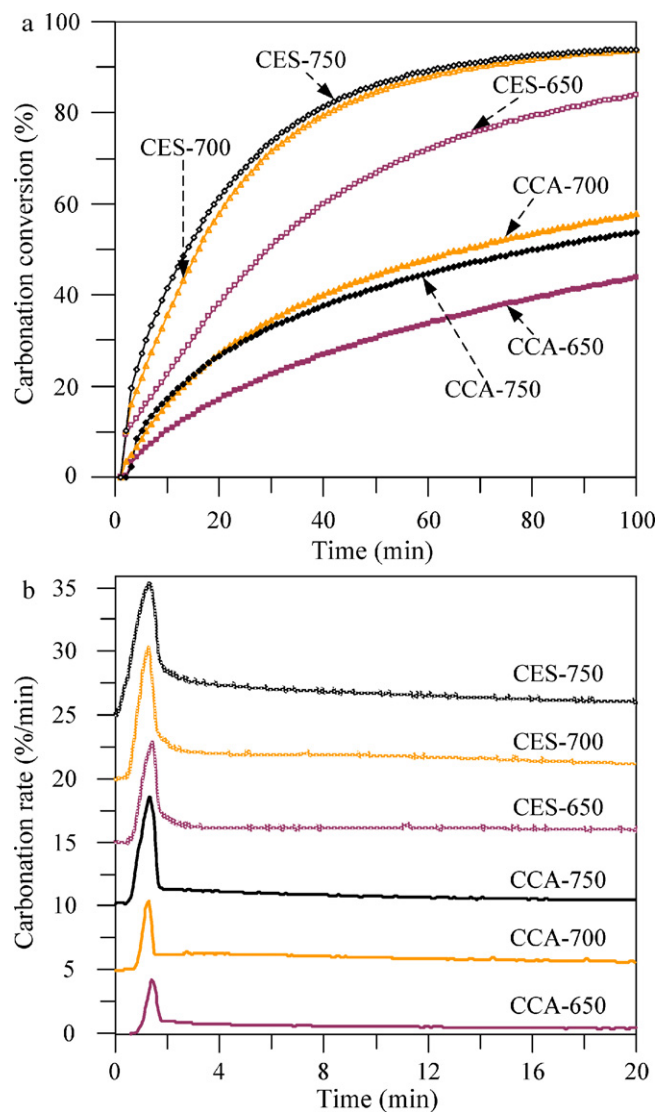


Fig. 6. Carbonation conversions (a) and carbonation rate (b) of calcined eggshell (CES) and calcined commercially available CaCO_3 (CCA) with different reaction temperatures after 1 cycle.

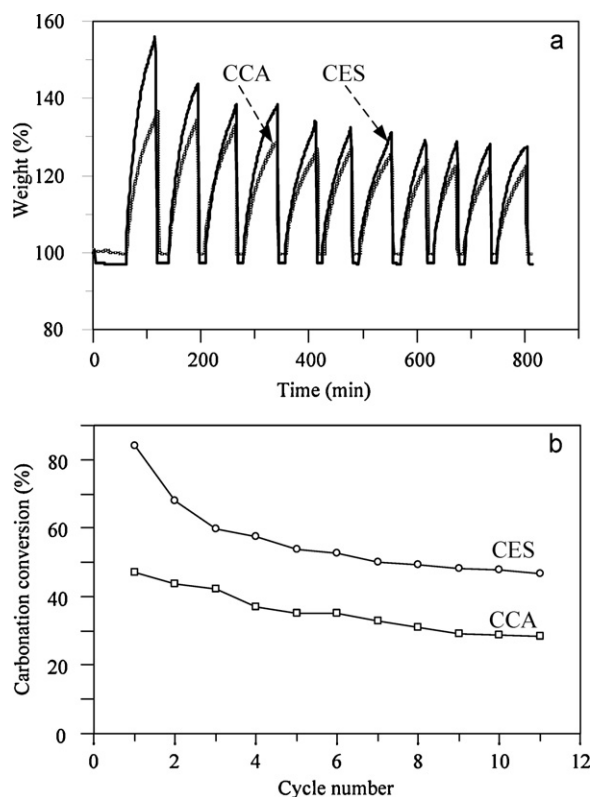


Fig. 7. Typical weight changes versus time from the TGA corresponding to carbonation–calcination through 11 cycles (a) and carbonation conversions with number of cycles (b) of calcined eggshell (CES) and calcined commercially available CaCO_3 (CCA).

available CaCO_3 (CCA), multiple carbonation cycles were performed and the results are presented in Fig. 7. Fig. 7a shows the typical data recorded in the computer in the form of weight changes over time in percentage of the CES and the CCA sorbents. It can be seen that the initial weight in percentage before the carbonation process of each sorbent is found to be different. This may be due to the presence of different amount of physically–chemically bound water. Therefore, the weight changes during carbonation–calcination steps were converted to the conversion with number of cycles based on Eq. (3) and the results are shown in Fig. 7b. It is obviously that the CO_2 capture capacity of the CES sorbent is higher than that of the CCA sorbent when compared at the same cycle. However, the CES sorbent displays a sharp decay in carbonation conversion from the first cycle to the third cycle. In contrast, the CCA sorbent showed a steady and much slower rate of decay. This observation can be explained by the fact that the smaller particle size of the CES sorbent is unstable and easier sintering during the carbonation–calcination steps which promote the formation of aggregated particles, resulting in the increase of particle size. The large particle size not only reduced an exposed surface area for the surface reaction of CO_2 but also increased the thickness of CaCO_3 layer for the CO_2 diffusion. Nevertheless, after 11 cycles, the carbonation conversion of the CES sorbent was 1.6 times as high as that of the CCA sorbent.

4. Conclusion

This work presents the characterization of the waste eggshell, the calcined eggshell (CES) and the calcined commercially available CaCO_3 (CCA) for the use as CO_2 sorbent. It is found that the CES is the major component of the CES sorbent. The CaO crystallite size and the CaO particle size of the CES sorbent are smaller than those of the CCA sorbent. The effect of temperature on the reaction between sorbents and CO_2 was investigated. The results showed that the suitable temperature for carbonation reaction is 700°C . The CO_2 capture capacity of the CES sorbent is higher than that of the CCA sorbent due to its smaller CaO particle size which provides a higher exposed surface for the surface reaction of CO_2 . This finding indicates that the CaO derived from the waste eggshell is attractive for the use as CO_2 sorbent due to its potentially low cost, environmentally benign nature and high CO_2 capture capacity.

Acknowledgements

This work is financially supported by the Thailand Research Fund (TRF-MRG54) (for Dr. Thongthai Wittoon), the Commission on Higher Education, Ministry of Education (the “National Research University Project of Thailand (NRU)”) and the “National Center of Excellence for Petroleum, Petrochemical and Advanced Materials (NCE-PPAM)”. Support from the Kasetsart University Research and Development Institute (KURDI) is also acknowledged.

References

- [1] S. Siitonen, P. Ahtila, The influence of operational flexibility on the exploitation of CO_2 reduction potential in industrial energy production, *J. Clean. Prod.* 18 (2010) 867–874.
- [2] J.A. Moya, N. Pardo, A. Mercier, The potential for improvements in energy efficiency and CO_2 emissions in the EU27 cement industry and the relationship with the capital budgeting decision criteria, *J. Clean. Prod.* 19 (2011) 1207–1215.
- [3] H. Chen, K. Cheng, F. Ye, W. Weng, Preparation and characterization of graded SSC-SDC MIEC cathode for low-temperature solid oxide fuel cells, *Ceram. Int.* 37 (2011) 1209–1214.
- [4] A.A. Olajire, CO_2 capture and separation technologies for end-of-pipe applications – a review, *Energy* 35 (2010) 2610–2628.
- [5] T. Wittoon, N. Tatan, P. Rattanavichian, M. Chareonpanich, Preparation of silica xerogel with high silanol content from sodium silicate and its application as CO_2 adsorbent, *Ceram. Int.* (2011), doi:10.1016/j.ceramint.2011.03.020.
- [6] World Nuclear Association (WNA), 2011. Available at: <http://www.world-nuclear.org/info/inf16.html> (accessed 07.05.11).
- [7] A.B. Rao, E.S. Rubin, A technical, economic, and environmental assessment of amine-based CO_2 capture technology for power plant greenhouse gas control, *Environ. Sci. Technol.* 36 (2002) 4467–4475.
- [8] R. Rivera-Tinoco, C. Bouallou, Comparison of absorption rates and absorption capacity of ammonia solvents with MEA and MDEA aqueous blends for CO_2 capture, *J. Clean. Prod.* 18 (2010) 875–880.
- [9] T. Harkin, A. Hoadley, B. Hooper, Reducing the energy penalty of CO_2 capture and compression using pinch analysis, *J. Clean. Prod.* 18 (2010) 857–866.
- [10] Norwegian Institute of Public Health, 2011. Available at: <http://www.biosciencetechnology.com/News/Feeds/2011/04/industries-CO2-capture-health-effects-of-amines-and-their-de/> (accessed 07.05.11).

- [11] V. Manovic, E.D. Anthony, CaO-based pellets supported by calcium aluminate cements for high-temperature CO₂ capture, *Environ. Sci. Technol.* 43 (2009) 7117–7122.
- [12] L. Li, D.L. King, Z. Nie, X.S. Li, C. Howard, MgAl₂O₄ spinel-stabilized calcium oxide adsorbents with improved durability for high-temperature CO₂ capture, *Energy Fuel* 24 (2010) 3698–3703.
- [13] N.H. Florin, A.T. Harris, Reactivity of CaO derived from nano-sized CaCO₃ particles through multiple CO₂ capture-and-release cycles, *Chem. Eng. Sci.* 64 (2009) 187–191.
- [14] C.H. Huang, K.P. Chang, C.-T. Yu, P.C. Chiang, C.F. Wang, Development of high-temperature CO₂ sorbents made of CaO-based mesoporous silica, *Chem. Eng. J.* 161 (2010) 129–135.
- [15] V. Manovic, E.D. Anthony, Reactivation and remaking of calcium aluminate pellets for CO₂ capture, *Fuel* 90 (2011) 233–239.
- [16] H. Chen, C. Zhao, L. Duan, C. Liang, D. Liu, X. Chen, Enhancement of reactivity in surfactant-modified sorbent for CO₂ capture in pressurized carbonation, *Fuel Process. Technol.* 92 (2011) 493–499.
- [17] C. Luo, Y. Zheng, N. Ding, Q. Wu, G. Bian, C. Zheng, Development and performance of CaO/La₂O₃ sorbents during calcium looping cycles for CO₂ capture, *Ind. Eng. Chem. Res.* 49 (2010) 11778–11784.
- [18] Y. Li, C. Zhao, H. Chen, L. Duan, X. Chen, Cyclic CO₂ capture behavior of KMnO₄-doped CaO-based sorbent, *Fuel* 89 (2010) 642–649.
- [19] L. Li, D.L. King, Z. Nie, X.S. Li, C. Howard, MgAl₂O₄ spinel-stabilized calcium oxide adsorbents with improved durability for high-temperature CO₂ capture, *Energy Fuel* 24 (2009) 3698–3703.
- [20] S.F. Wu, Y.Q. Zhu, Behavior of CaTiO₃/nano-CaO as a CO₂ reactive adsorbent, *Ind. Eng. Chem. Res.* 49 (2010) 2701–2706.
- [21] A. Silaban, M. Narcida, D.P. Harrison, Characteristics of the reversible reaction between CO₂(g) and calcined dolomite, *Chem. Eng. Commun.* 146 (1996) 149–162.
- [22] J.J. Klemeš, P.S. Varbanov, S. Pierucci, D. Huisinigh, Minimising emissions and energy wastage by improved industrial processes and integration of renewable energy, *J. Clean. Prod.* 18 (2010) 843–847.
- [23] M.V. Iyer, L.-S. Fan, High temperature CO₂ capture using engineered eggshells: a route to carbon management, Patent No. US 76,787,351 B2 (2010).
- [24] A. Doostmohammadi, A. Monshi, M.H. Fathi, Z. Golniya, A.U. Daniels, Bioactive glass nanoparticles with negative zeta potential, *Ceram. Int.* (2011), doi:10.1016/j.ceramint.2011.03.026.
- [25] G. Gergely, F. Wéber, I. Lukács, A.L. Tóth, Z.E. Horváth, J. Mihály, C. Balázs, Preparation and characterization of hydroxyapatite from eggshell, *Ceram. Int.* 36 (2010) 803–806.



Thongthai Witoon, D. Eng. is a lecturer at the Department of Chemical Engineering Kasetsart University, Thailand. He received the Scholarship from the Royal Golden Jubilee (RGJ) Program under the Thailand Research Fund (TRF) for doctoral degree study in Kasetsart University. His research focuses are mainly on the nanomaterials synthesis using renewable resources, the CO₂ capture at low and high temperature and the fine chemical production from CO₂ hydrogenation reaction. His works have been appeared in international journals including *Materials Letters*, *Journal of Sol–Gel Science Technology*, *Colloids and Surfaces A: Physicochemical and Engineering Aspects*, *Fuel Processing Technology* and *Ceramics International*.